



# THE UNIVERSITY *of* EDINBURGH

## Edinburgh Research Explorer

### Assessment of a pulsating torque mitigation control strategy through tidal turbine emulation

**Citation for published version:**

Sousounis, MC & Shek, JKH 2019, 'Assessment of a pulsating torque mitigation control strategy through tidal turbine emulation', *Journal of Engineering*, vol. 2019, no. 18, pp. 5059-5063.  
<https://doi.org/10.1049/joe.2018.9306>

**Digital Object Identifier (DOI):**

[10.1049/joe.2018.9306](https://doi.org/10.1049/joe.2018.9306)

**Link:**

[Link to publication record in Edinburgh Research Explorer](#)

**Document Version:**

Early version, also known as pre-print

**Published In:**

Journal of Engineering

**General rights**

Copyright for the publications made accessible via the Edinburgh Research Explorer is retained by the author(s) and / or other copyright owners and it is a condition of accessing these publications that users recognise and abide by the legal requirements associated with these rights.

**Take down policy**

The University of Edinburgh has made every reasonable effort to ensure that Edinburgh Research Explorer content complies with UK legislation. If you believe that the public display of this file breaches copyright please contact [openaccess@ed.ac.uk](mailto:openaccess@ed.ac.uk) providing details, and we will remove access to the work immediately and investigate your claim.



# Assessment of a pulsating torque mitigation control strategy through tidal turbine emulation

*M.C. Sousounis\*, J.K.H. Shek*

*School of Engineering, Institute for Energy Systems, The University of Edinburgh, Faraday Building, King's Buildings, Colin Maclaurin Road, Edinburgh EH9 3DW, UK, \*[M.Sousounis@ed.ac.uk](mailto:M.Sousounis@ed.ac.uk)*

**Keywords:** Turbine emulation, tidal energy, fatigue reduction, control strategy.

## Abstract

This paper presents the modelling and assessment of a pulsating torque mitigation control strategy by using a tidal turbine emulator in a laboratory environment. Sudden changes and variability of the tidal flow velocity have the effect of creating pulsations on tidal current turbines. These pulsations have an adverse effect on tidal turbine fatigue and ultimate loading as well as the operation of the drivetrain. For the above reasons a pulsating torque mitigation control strategy has been developed and tested which is based on modifying the reference maximum power point speed of the generator. This paper presents the assessment of this pulsating torque mitigation control strategy in a laboratory setup. A 7kW tidal current turbine is modelled in MATLAB/Simulink. The tidal turbine is emulated in the laboratory setup by using a torque-controlled induction motor. Results show the effectiveness of the method in a laboratory environment, the ability of the generator to accelerate and decelerate based on the speed controller commands and the difference between the pulsating torque mitigation control strategy and maximum power point operation. In addition, the experimental results are compared with a Simulink model which will show the accuracy of the modelling process.

## 1 Introduction

A number of tidal current developers are planning or have installed demonstration arrays with a notable example the MeyGen project in the Inner Sound of the Pentland Firth in Scotland. Based on [1] for the Phase 1A of the MeyGen project four 1.5MW horizontal-axis three-bladed tidal current turbines with pitch control were deployed. Phase 1B will involve the installation of an additional four 1.5MW turbines while Phase 1C aims to add 73.5MW at MeyGen with the project commencing in 2019. However, the tidal current industry in the UK is competing against offshore wind which is a more established technology with lower levelised cost of energy (LCOE). A significant reduction of the LCOE can be achieved by reducing unexpected maintenance and increase the lifetime of critical components in a tidal current conversion system. It is for this purpose that a novel speed based fatigue load reduction control strategy is proposed for tidal current turbines in [2].

The high energy density of the tidal currents can lead to significant amounts of power but at the same time subject the tidal current turbine to large thrust forces and blade torque loads. What is more, the flow of the tidal currents is unsteady with high variations due to shear flow [3], waves [4] and turbulence [3]. Peak loads and thrust forces are usually limited by setting a maximum power the tidal turbine can capture. In [5] the performance of stall and pitch regulated tidal current turbines are compared. Authors conclude that a pitch-to-feather control system is more stable in regulating the maximum power and had lower out-of-plane bending moments at above rated power operation.

For below rated power operation however, variations of the forces and the torque on a tidal current turbines have to be minimised in order to avoid blade lifetime reduction, unnecessary use of the pitching system and gearbox stress. Most research focuses on reducing torque and force variations on turbines by designing the blades in different ways. Cutting edge research uses individual blade pitching as the one presented in [6] to mitigate fatigue and ultimate loads on the blades or fatigue loads on the hub and tower structure. The use of individual blade pitching requires specific load measurements from the blades which is a disadvantage since the effectiveness of the individual blade pitching is sensitive to these measurements being correct. An additional disadvantage of the individual blade pitching method is the potential over-usage of the pitching system. According to [7] and [8] the frequency converter, the blades and the pitch system are among the components in a renewable energy system that have both high failure rates and longer downtime for repair. Assuming that horizontal-axis tidal current systems will have similar reliability data to wind turbine systems, the frequency converter problem was addressed in [9] by using onshore converters connected to the generator through long subsea cables. The fatigue torque mitigation (FTM) control strategy using the speed controller was first presented in [2] together with an ultimate torque reduction method for peak load reduction. By reducing mechanical torque variations through the speed controller of the generator and applying appropriate pitch control for the above rated power operation the unnecessary use of the pitching system can be avoided and the failure rates of the mechanical parts of the turbines minimised. In this paper a tidal current turbine is emulated in real time in the laboratory environment through a torque-controlled induction motor. The shaft of the induction motor is connected to the generator whose speed is controlled using an active rectifier. The speed reference for the active rectifier is

generated in real time depending on the control method selected which is either maximum power point operation (MPPO) or FTM.

The paper has the following structure. First, the laboratory test-rig and the model of the tidal current turbine developed in MATLAB/Simulink is described in Section 2. In Section 3 the experimental results are assessed and compared with the simulation model. In addition, the effectiveness of the FTM control strategy is presented and assessed compared to the MPPO control strategy. Finally, in Section 4 conclusions are derived.

## 2 Tidal turbine emulation

In this Section the laboratory setup will be described along with the simulation model of the 7kW tidal current conversion system. Figure 1a shows the block diagram of the laboratory setup for the tidal turbine emulation. Figure 1b depicts the tidal current conversion system as in Figure 1a modelled in SimPowerSystems.

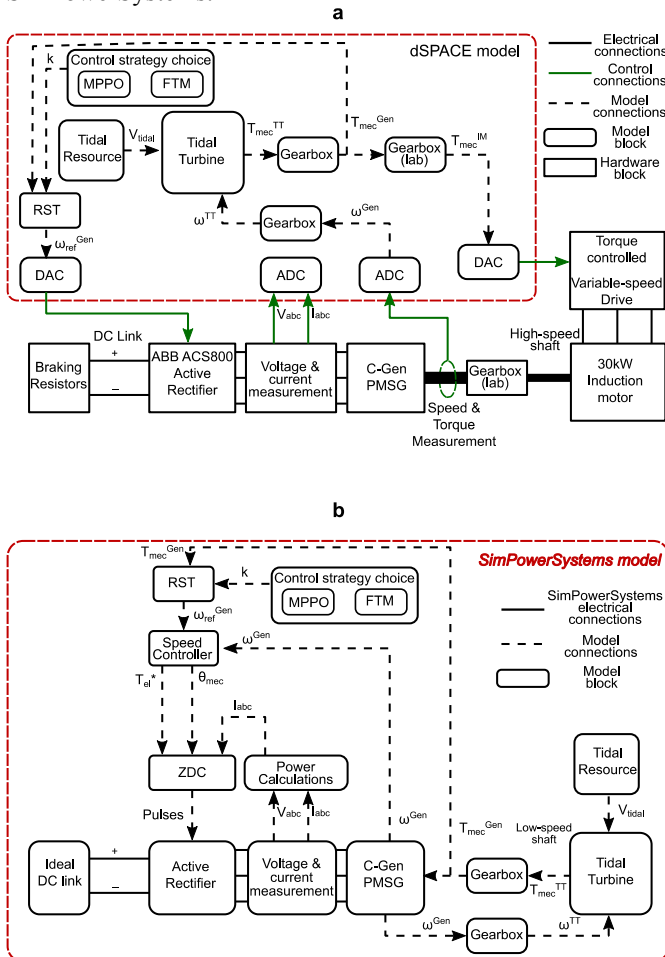


Figure 1: a. Tidal turbine emulator laboratory setup. b. Simulink SimPowerSystems model.

In Figure 1a the tidal turbine emulation is achieved through the torque controlled variable-speed drive. As shown in Figure 1b the tidal turbine is connected to the C-Gen PMSG through a Gearbox. This is to decrease the speed of the high speed shaft

of the generator  $\omega^{Gen}$  to the low speed shaft of the tidal turbine  $\omega^{TT}$ . The reverse process is followed for the torque, the  $T_{mec}^{TT}$  is decreased to  $T_{mec}^{Gen}$  using the Gearbox. In the laboratory setup however there is an additional gearbox, the Gearbox(lab) that has to be considered. The induction motor that is operated in torque controlled mode is connected to the C-Gen PMSG through the Gearbox(lab). Therefore the command to the torque controlled variable-speed drive (SSD drive) is  $T_{mec}^{IM}$  so that at the point where speed and torque is measured the torque applied to the generator shaft is  $T_{mec}^{Gen}$ .

At this point it has to be noted that all the necessary conversions and scaling were performed in order to convert the signals from digital-to-analogue (DAC) and analogue-to-digital (ADC). The torque command  $T_{mec}^{IM}$  is converted to percentage value of the induction motor rated torque and scaled as a voltage signal. The  $\omega_{ref}^{Gen}$  signal was scaled according to the requirements of ABB ACS800-01 drive to a voltage signal. The speed at the C-Gen PMSG shaft was measured as a square wave pulse whose frequency was the speed of the generator shaft,  $\omega^{Gen}$ , in rpm. Finally, voltages and currents were measured at the output of the C-Gen PMSG for monitoring.

The laboratory setup equipment can be seen in Figure 2.



Figure 2: Experimental setup in the laboratory.

The design, building process and advantages of the C-Gen PMSG are described in [10] in detail. The 'C' core concept is used to design air-cored permanent magnet synchronous machines (PMSM). This concept offers reduced mass for PMSM due to the absence of iron in the stator and modularity using both the 'C' core rotor modules and stacking of machines with the same radius axially. These features can provide easy maintenance and assembly as well as fault tolerance which are

all attractive concepts for the inherently inaccessible tidal current conversion systems. The ABB ACS800-01 drive is primarily designed to drive motors and therefore the drive does not have the ability to supply the power to the grid. For that purpose the drive was operated in resistive braking mode by enabling the braking chopper. The generated energy was dissipated as heat to the braking resistors and the voltage at the DC link of the ABB drive was kept relatively constant at 675V. The two braking resistors (MFPR) seen in Figure 2 were connected in parallel forming a total resistance of 48Ω and total power of 14kW. The ABB ACS800-01 drive has an integrated speed controller and therefore only the reference speed  $\omega_{ref}^{Gen}$  was required as input to the drive. Based on this input the ABB drive was generating the appropriate pulses for the active rectifier. This process was modelled in the SimPowerSystems model by using a speed controller and implementing the zero d-axis controller (ZDC) for PMSM. Finally the dSPACE DS1103 controller was used to run the SimPowerSystem models in real time, convert the digital signals from the model to appropriate voltage signals for the controllers and save the experimental results. Both models of Figure 1, the dSPACE model and the SimPowerSystems model, were loaded in the dSPACE controller and ran in parallel in real time in order to compare the results. The whole experimental process was monitored and controlled using the ControlDesk which acts as an interface between Simulink and the dSPACE controller.

## 2.1 The tidal turbine design

The tidal current turbine model converts the tidal current velocity input to mechanical power for the generator rotor based on equations (1) and (2). The output of the tidal current turbine is mechanical torque,  $T_{mec}^{TT}$ , which is used as input to the generator after the gearbox ratio is considered (Figure 1).

$$P_{mec}^{TT} = \frac{1}{2} \times \rho_{water} \times A \times C_p(\lambda, \beta) \times V_{tidal}^3 \quad (1)$$

$$T_{mec}^{TT} = P_{mec}^{TT} / \omega_{mec}^{TT} \quad (2)$$

The tidal current turbine used in this paper is a hypothetical three-bladed horizontal-axis 7kW turbine. The numerical tool of Harp\_Opt [11] was used which combines blade element momentum theory with a genetic algorithm to generate a structurally optimised blade design. From the outputs of Harp\_Opt the  $C_p$  curve of the turbine as well as turbine inertia and gearbox ratio were calculated. The tidal current turbine specifications used are given in Table 1 and the  $C_p(\lambda)$  curve in Figure 3.

Parameter	Value	Units
Rated power, $P^{TT}$	7	kW
Rotor diameter, $R^{TT}$	5	m
Hub diameter	0.7	m
Maximum $C_p$	0.41	-
Optimum $\lambda$	3.1	-
Base tidal flow speed	1.2	m/s
Inertia, $J$	490	kg.m <sup>2</sup>
Gearbox ratio, $N_{gb}$	4.1	-
Gearbox (lab) ratio	13.8	-

Table 1: Specifications for the tidal turbine and its emulation.

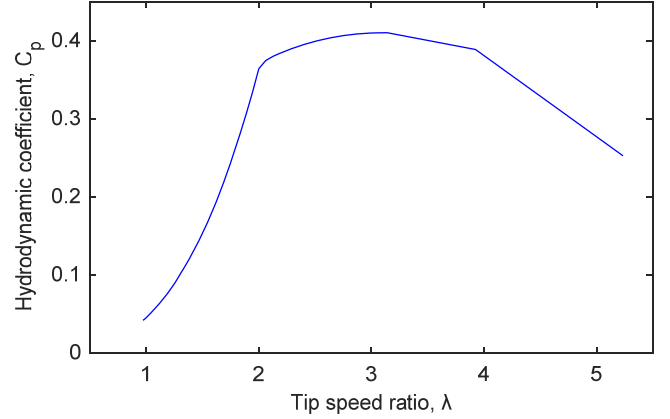


Figure 3: Hydrodynamic coefficient of the tidal current turbine modelled.

The tip speed ratio (TSR) or  $\lambda$  is calculated using equation (3).

$$\lambda = \frac{\omega^{TT} \times R^{TT}}{V_{tidal}} \quad (3)$$

Even though a pitch control system was modelled it is not included in the analysis because all the experiments were performed at below rated values.

## 2.2 Reference speed tracking

The reference speed tracking block (RST) generates the appropriate reference speed signal,  $\omega_{ref}^{Gen}$ , for the speed controller depending on the input  $k$  and the mechanical torque at the generator shaft. The equation of the reference speed tracking is based on (4).

$$\omega_{ref}^{Gen} = \sqrt{\frac{T_{mec}^{Gen}}{k^2}} \quad (4)$$

## 2.3 Maximum power point operation

The maximum power point operation (MPPO) strategy has one major aim: to control the tidal turbine's  $\lambda$  in order to achieve the highest possible  $C_p$ . Based on the data presented in Table 1 the optimum  $\lambda$  is 3.1. In order to achieve that,  $\omega^{TT}$  has to change as  $V_{tidal}$  changes so that  $\lambda$  in equation (3) remains constant. This is achieved by calculating an appropriate value for  $k$  described in equation (4) which will generate an appropriate  $\omega_{ref}^{Gen}$  signal for the speed controller. In equation (4) the changes in tidal current speed are monitored through  $T_{mec}^{Gen}$ . The value of  $V_{tidal}$  could also be used and appropriate generated torque could be estimated through calculation using equations (1) and (2). There are many different ways of calculating the appropriate value for  $k$  in order to achieve MPPO. In [12] authors explore different ways to control a vertical-axis tidal current conversion system in a laboratory setup as well as giving an equation for calculating  $k$ . In this paper  $k_{MPPO}$  was calculated based on equation (5):

$$k_{MPPO} = \sqrt{\frac{P^{TT}}{\omega_{rated}^{TT}{}^3}} / N_{gb}^2 = 3.6684 \quad (5)$$

Based on equations (1) and (5) we can visualise the power output of the tidal turbine for different  $V_{tidal}$  and  $\omega^{TT}$ .

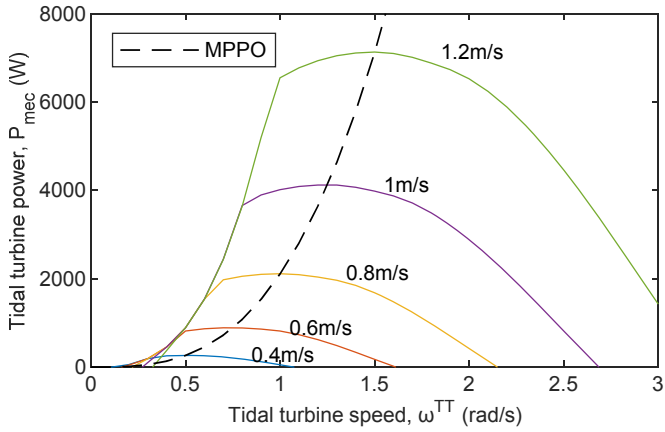


Figure 4: Tidal turbine power curves versus speed for different tidal current velocities. The maximum power point operation is also depicted.

## 2.4 Fatigue torque mitigation

The FTM control strategy was first described in [2]. In order to mitigate torque pulsations, either sudden flow velocity changes or fatigue torque, the control methodology of MPPO has to be modified. In the FTM, this is achieved by modifying the coefficient  $k$  and therefore forcing the generator to follow a different reference speed with the aim of reducing torque variations. Coefficient  $k$  changes to lower and higher values depending on the difference between actual mechanical torque input,  $T_{mec}^{Gen}$ , and reference mechanical torque,  $T_{ref}^{Gen}$ . When  $T_{mec}^{Gen}$  is higher compared to  $T_{ref}^{Gen}$  coefficient  $k$  is increased so that the generator over-speeds and lowers the  $C_p$  value. When  $T_{mec}^{Gen}$  is lower compared to  $T_{ref}^{Gen}$  the generator under-speeds and puts the tidal current system in a state similar to regenerative braking. The maximum and minimum allowable values of coefficient  $k_{FTM}$  are depicted in Figure 5.

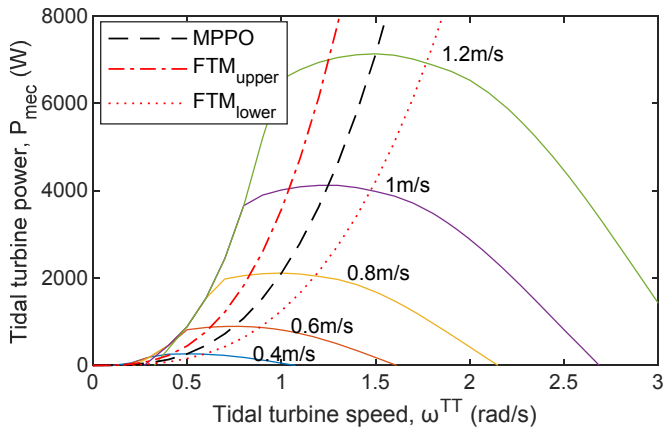


Figure 5: Tidal turbine power curves versus tidal turbine speed for different tidal current velocities. The maximum and minimum limits of  $k$  are shown for the FTM control strategy compared to the constant  $k$  for MPPO strategy.

The  $FTM_{upper}$  and  $FTM_{lower}$  has to be kept within the stable region of the power curves. If the FTM method reduces  $\omega^{TT}$  significantly then the TSR can drop below 2 (Figure 3) which will mean that a small reduction in  $\omega^{TT}$  will result in a

significant reduction of  $C_p$  and therefore power. This can cause the tidal current conversion system to become unstable. The same can happen if the FTM control method forces the system to operate at high TSR. The block diagram of the FTM control strategy is shown in Figure 6.

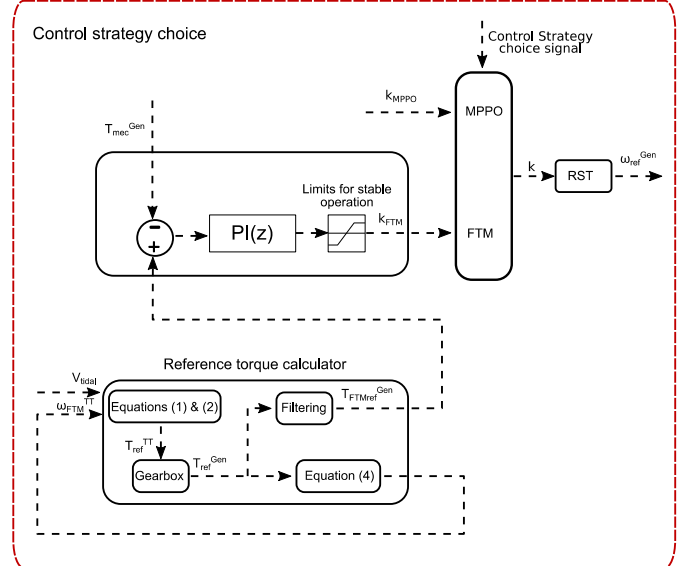


Figure 6: Block diagram of the FTM control strategy.

## 3 Results and discussion

The tidal current turbine system developed was emulated in the laboratory setup for two different test cases in order to assess the performance of the FTM control strategy compared to the MPPO control strategy. At the same time that the experimental setup was operating, the SimPowerSystems Simulink model was also simulated in real time with the same  $V_{tidal}$ . This is necessary in order to compare simulation and experimental results and understand possible limitations of the control strategy in the laboratory setup.

### 3.1 Test case 1: Sinusoidal flow

In the first test case a simple sinusoidal flow was used as input. Figure 7 presents the experimental and simulated results of the first test case.

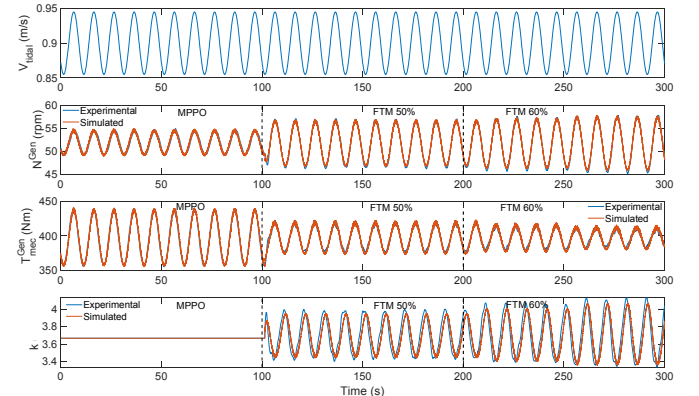


Figure 7: Comparison of experimental and simulated data for a sinusoidal flow speed input. The FTM control strategy is enabled in real time after 100 seconds of operation under the MPPO control strategy.

The tidal current velocity presented in Figure 7 has a mean value of 0.9m/s and varies about 0.09m/s with a period of 10s. This means that within 5s the tidal current speed goes from 0.855m/s to 0.945m/s. This tidal current velocity variation is used in order to represent the effect of waves in tidal current velocity. Observing Figure 7 it can be seen that the simulation model of the tidal current system presented in Figure 1b matches the experimental results acquired using the laboratory setup of Figure 1a. There are some variations mainly that the experimental results of generator speed in rpm ( $N^{Gen}$ ) and  $k$  have higher peak values compared to the simulated results and experimental torque peaks are slightly lower compared to the simulated torque peaks. In addition to the comparison between experimental and simulated results Figure 7 shows the differences between MPPO and FTM operation. Between 0 and 100s the system operates at MPPO, between 100s and 200s the system operates at FTM 50% and between 200s and 300s at FTM 60%. The percentage term in FTM shows the expected reduction in torque variation which was changed in real time in this test case. A general observation is that the torque variation has changed from 85Nm during MPPO to 42Nm during FTM 50% and to 30Nm during FTM 60%. The opposite has occurred for the  $N^{Gen}$ . Generator speed variation has increased from 5.17rpm during MPPO to 10.23rpm during FTM 50% and to 12.49rpm during FTM 60%. The average electrical power generated during MPPO was 3.095kW which is slightly higher compared to the 3.091kW and 3.089kW for the FTM 50% and FTM 60% respectively. In Figure 8 a closer look at the experimental results of MPPO, FTM 50% and FTM 60% is taken.

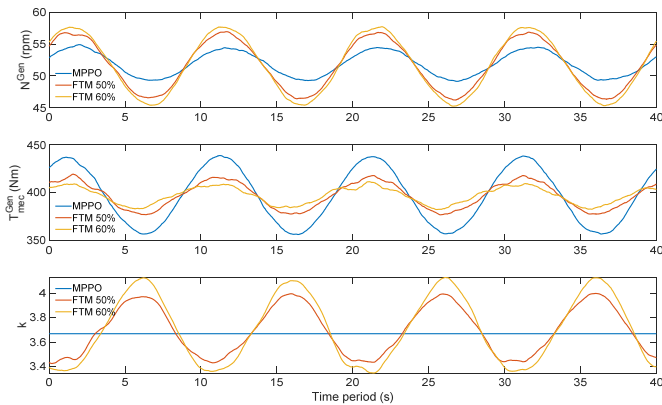


Figure 8: Synchronised experimental results for the three different operating conditions of the tidal current system, MPPO, FTM 50% and FTM 60%.

Figure 8 presents experimental results for generator speed, mechanical torque at the generator and coefficient  $k$  synchronised over a 40s period. Observing Figure 8 it can be seen that the mechanical torque input variation is significantly reduced when using the FTM method. The disadvantage of the FTM method is that it requires larger variations of generator speed. This requires the generator to accelerate and decelerate faster which can cause the speed controller to operate at its limits regarding the maximum change in speed per second. In the experiments for this paper the maximum acceleration and deceleration was 10rpm/s. In addition to generator speed and torque, the variation of coefficient  $k$  can be observed in Figure

8. During MPPO the coefficient remains constant as discussed in Section 2.3. When the FTM control method is enabled the coefficient  $k$  varies depending on the error torque as shown in Figure 6. During the FTM 50% coefficient  $k$  has a sinusoidal profile as expected. However, during FTM 60% the coefficient is saturated at some instances, for example at 36s in Figure 8, due to the constraints for stable operation discussed in Section 2.5. In order to assess the FTM control method the rainflow command for fatigue analysis from MATLAB is used. The rainflow command counts the number of cyclical load changes as a function of their amplitude. The rainflow counting on the generator torque for the time periods given in Figure 8 is presented in Figure 9.

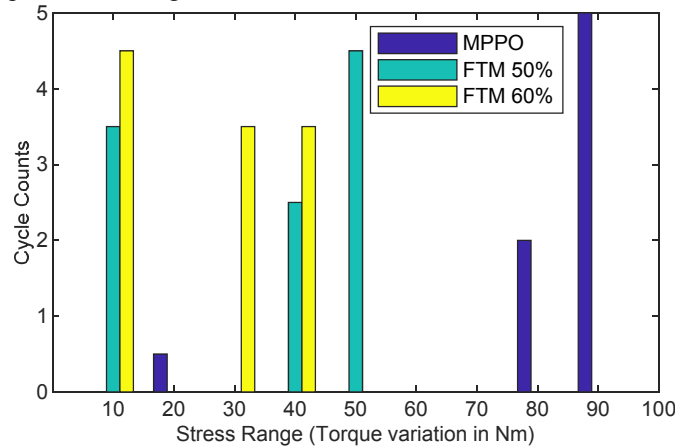


Figure 9: Rainflow counting for fatigue analysis for the three different operating conditions of the experimental setup. The stress range bins include all torque variations from the previous bin value up to the range indicated. Minimum torque variation considered was 1Nm.

Figure 9 shows the reduction in the stress range from the 80 and 90 bins during MPPO to the 40 and 50 bins for the FTM 50% and to the 30 and 40 bins during the FTM 60%.

### 3.2 Test case 2: Complex flow

In the second test case a complex flow composed from three sinusoidal frequencies was used as input. Figure 10 presents the experimental and simulated results of the second test case.

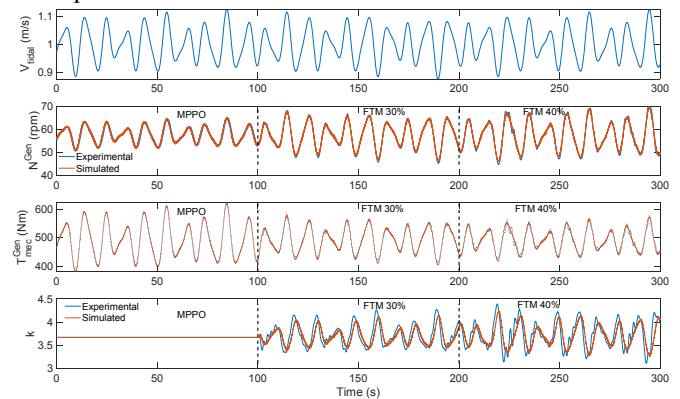


Figure 10: Comparison of experimental and simulated data for a complex flow velocity input.

Results from Figure 10 show that experimental and simulated data agree. Some errors between the data appears after the 200s when the FTM 40% is enabled. Some oscillations of the coefficient  $k$  affect the speed and torque of the system. These oscillations are caused due to the response of the speed controller of the ABB drive in the fast changes of the flow. Optimal tuning of the speed controller may reduce these oscillations but the tuning process of the speed controller and the FTM controller as an inner and outer control loop will be discussed in future work. The complex flow case is difficult to assess and synchronise between the different operating strategies and that is why the rainflow command for fatigue analysis is performed in Figure 11.

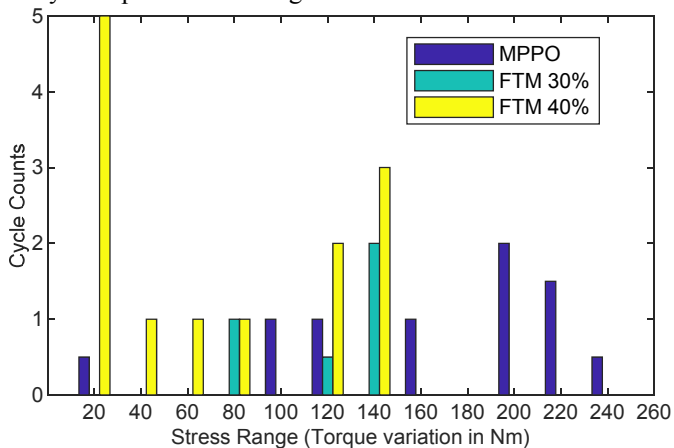


Figure 11: Rainflow counting for fatigue analysis for the three different operating conditions of the experimental setup using complex flow. Minimum torque variation considered was 5Nm.

Figure 11 shows the reduction in the stress range from the 200 to 240 bins during MPPO to the 120 and 140 bins for the FTM 30% and FTM 40%. It can also be observed that the FTM 40% does reduce the stress range compared to FTM 30%. This is due to the oscillations of coefficient  $k$  as described in Figure 10.

## 4 Conclusions

In this paper a tidal current turbine was emulated in the laboratory environment in order to assess a novel control strategy that aims to reduce torque pulsations. By testing the system under two different cases it was identified that the FTM control strategy reduces the stress range compared to the MPPO strategy which is widely used. The reduction in the torque variations comes with similar electrical power generated but increased speed variations. In addition to the assessment of the control strategy, the experimental results were compared to simulated results from a SimPowerSystems model. This showed that the results between the laboratory setup and the simulation model agree. The FTM control strategy assessed in this paper can potentially benefit tidal current turbines by increasing the lifetime of the mechanical components without affecting generated power.

## Acknowledgements

The authors would like to acknowledge the support of the EPSRC in funding the work within this paper (EP/N035593).

## References

- [1] Atlantis Resources Ltd: 'MeyGen', <https://www.atlantisresourcesltd.com/projects/meygen/>, accessed May 2018
- [2] Sousounis, M.C., Shek, J.K.H.: 'Mitigation of Torque Pulsations in Variable Pitch Tidal Current Turbines Using Speed Control', in 'Proceedings of the 12th European Wave and Tidal Energy Conference' (2017), pp. 1146-1-9
- [3] Afgan, I., McNaughton, J., Rolfo, S., Apsley, D.D., Stallard, T., Stansby, P.: 'Turbulent flow and loading on a tidal stream turbine by LES and RANS' *Int. J. Heat Fluid Flow*, 2013, **43**, pp. 96-108.
- [4] Luznik, L., Flack, K.A., Lust, E.E., Taylor, K.: 'The effect of surface waves on the performance characteristics of a model tidal turbine' *Renew. Energy*, 2013, **58**, pp. 108-114.
- [5] Whitby, B., Ugalde-Loo, C.E.: 'Performance of Pitch and Stall Regulated Tidal Stream Turbines' *IEEE Trans. Sustain. Energy*, 2014, **5**, (1), pp. 64-72.
- [6] Han, Y., Leithead, W.E.: 'Combined wind turbine fatigue and ultimate load reduction by individual blade control' *J. Phys. Conf. Ser.*, 2014, **524**, (012062), pp. 1-10.
- [7] Uzunoglu, B., Amoiralis, F., Kaidis, C.: 'Wind turbine reliability estimation for different assemblies and failure severity categories' *IET Renew. Power Gener.*, 2015, **9**, (8), pp. 892-899.
- [8] Carroll, J., McDonald, A., McMillan, D.: 'Failure rate, repair time and unscheduled O&M cost analysis of offshore wind turbines' *Wind Energy*, 2016, **19**, (6), pp. 1107-1119.
- [9] Sousounis, M.C., Shek, J.K.H., Mueller, M.A.: 'Modelling, control and frequency domain analysis of a tidal current conversion system with onshore converters' *IET Renew. Power Gener.*, 2016, **10**, (2), pp. 158-165.
- [10] Mueller, M.A., McDonald, A.S.: 'A lightweight low-speed permanent magnet electrical generator for direct-drive wind turbines' *Wind Energy*, 2009, **12**, (8), pp. 768-780.
- [11] 'NWTC Information Portal (HARP\_Opt)', [https://nwtc.nrel.gov/HARP\\_Opt](https://nwtc.nrel.gov/HARP_Opt), accessed March 2018
- [12] Cavagnaro, R.J., Neely, J.C., Fay, F.-X., Mendia, J.L., Rea, J.A.: 'Evaluation of electromechanical systems dynamically emulating a candidate hydrokinetic turbine' *IEEE Trans. Sustain. Energy*, 2016, **7**, (1), pp. 390-399.